XLI CILAMCE
XLI Ibero-Latin American Congress on Computational Methods in Engineering
16-19 November, 2020 FOZ DO IGUAÇU PARANÁ - BRAZIL

A simple fully nonlinear Kirchhoff-Love shell finite element

Matheus L. Sanchez[1], Catia C. Silva[1], Paulo M. Pimenta[1]

[1] *Polytechnic School at University of São Paulo*
Av. Prof. Almeida Prado, trav.2 nº. 83 Edifício Paula Souza, 05424-970, São Paulo, Brazil
matheus.sanchez@usp.br, catia1@usp.br, ppimenta@usp.br

Abstract. The current work develops a new simple Kirchhoff-Love shell finite element model for reliable and efficient simulation of thin nonlinear structures. This new shell triangular element has 6 nodes and uses penalty methods to approximate displacement C^1 continuity. The DOF's are the displacements u at the six nodes and an incremental scalar rotation parameter φ_Δ at mid-side nodes. The incremental rotation vector α_Δ (incremental Rodrigues parameters) and incremental rotation tensor Q at the mid-side nodes are computed at element level by solving simple equations. The displacements "u" are interpolated by quadratic polynomials from the nodal values as usual. Simulations are done comparing its results to other numerical models in order to verify model reliability.

Keywords: Finite Element Method, Kirchoff Love shell, Non-linear

1 Introduction

The model developed in this work aims to be a good alternative for simulation of nonlinear thin shells with finite element method. Shell mechanics is an import topic of study once it is very applicable in engineering. Important work has been done in this field (shell + computational mechanics) by Simo JC [1] and Pimenta [2] before 2000's and later by Campello et al. [3], Viebahn et al. [4] and Costa e Silva [5]. It is shown in the bibliography that if not simulated properly, thin structures may present locking phenomena (structure seems stiffer than what it really is) may occur. This is the main motivation for many researches in shell computational mechanics. Given that, the present work continues the models developed by Viebahn et al. [4] and Costa e Silva [5]. Further information may be checked in a forthcoming article Sanchez et al. [6].

2 Model Description

Shell Kinematics

The model presented in this paper is based on Kirchhoff-Love shell kinematics, also known as Classical Shell/Plate theory (Reddy [7]). The main kinematic restrictions which the shells are subject in this theory are:

1. Straight perpendicular lines to the middle surface stay straight after any deformation.
2. The same straight perpendicular lines don't change its length, i.e., they are inextensible.
3. The same straight perpendicular lines remain perpendicular to the middle surface during any deformation imposed to the shell.

Figure 1 illustrates the kinematical model used. A plane initial configuration is assumed, even though curved shells may be represented as an initial stress-free deformation (Pimenta et al. [8]).

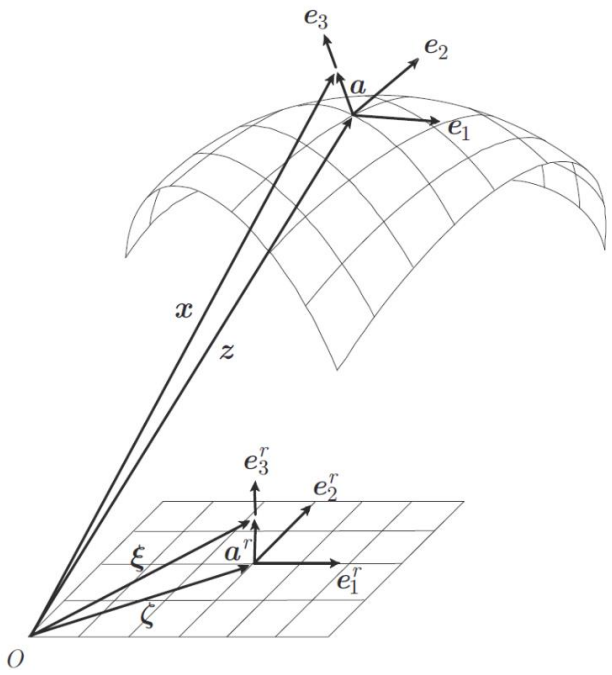

Figure 1. Shell kinematical model.

The kinematical model is based on the article Pimenta et al [9] and the FEM model is better explained in Sanchez et al. [6]. The position of an arbitrary point in the shell is defined by vector $\boldsymbol{x} \in \mathbb{R}^3$ in the current configuration. Its counterpart in the reference configuration is $\boldsymbol{\xi} \in \mathbb{R}^3$. These position vectors may be divided in two components: by its projection to shell middle surface ($\boldsymbol{z} \in \Omega \subset \mathbb{R}^3$ and $\boldsymbol{\zeta} \in \Omega^r \subset \mathbb{R}^2$ in the current and reference configurations respectively) and a perpendicular vector to this surface ($\boldsymbol{a}$ and $\boldsymbol{a^r}$). The following equations resumes the shell kinematics

$$\boldsymbol{\xi} = \boldsymbol{\zeta} + \boldsymbol{a^r} \quad , \quad \boldsymbol{\zeta} = \xi_\alpha \boldsymbol{e_\alpha^r},\ \xi_\alpha \in \Omega^r \quad , \quad \boldsymbol{a^r} = \xi_3 \boldsymbol{e_3^r},\ \xi_3 \in H^r \ , \tag{1}$$

$$\boldsymbol{z} = \boldsymbol{\zeta} + \boldsymbol{u} \quad , \quad \boldsymbol{a} = \boldsymbol{Q a^r} \quad \text{and} \quad \boldsymbol{x} = \boldsymbol{z} + \boldsymbol{a} \ . \tag{2}$$

The rotation tensor $\boldsymbol{Q}$ and the derivatives of $\boldsymbol{z}$ are defined as

$$\boldsymbol{Q} = \boldsymbol{e_i} \otimes \boldsymbol{e_i^r} \ , \quad \boldsymbol{z}_{,\alpha} = \frac{\partial(\xi_\alpha \boldsymbol{e_\alpha^r} + \boldsymbol{u})}{\partial \xi_\alpha} = \boldsymbol{e_\alpha^r} + \boldsymbol{u}_{,\alpha} \quad \text{and} \quad \boldsymbol{z}_{,\alpha\beta} = \boldsymbol{u}_{,\alpha\beta} \quad \text{where} \quad (\cdot)_\alpha = \frac{\partial(\cdot)}{\partial \xi_\alpha}. \tag{3}$$

The deformation gradient $\boldsymbol{F}$ is defined by

$$\boldsymbol{F} = \partial \boldsymbol{x} / \partial \xi = \frac{\partial(\boldsymbol{z} + \boldsymbol{Q a^r})}{\partial \xi_\alpha} \otimes \boldsymbol{e_\alpha^r} + \frac{\partial(\boldsymbol{z} + \boldsymbol{Q a^r})}{\partial \xi_3} \otimes \boldsymbol{e_3^r} = \boldsymbol{f_\alpha} \otimes \boldsymbol{e_\alpha^r} + \boldsymbol{f_3} \otimes \boldsymbol{e_3^r} \, , \tag{4}$$

and the curvature vectors are defined as

$$\boldsymbol{K_\alpha} = \boldsymbol{Q}_{,\alpha} \boldsymbol{Q^T} \quad \text{and} \quad \boldsymbol{\kappa_\alpha} = axial(\boldsymbol{K_\alpha}) \, . \tag{5}$$

With previous equation, components of deformation gradient may be rewritten and the jacobian defined as

$$\boldsymbol{f_\alpha} = \boldsymbol{z}_{,\alpha} + \boldsymbol{\kappa_\alpha} \times \boldsymbol{a} \quad \text{and} \quad J = det\, \boldsymbol{F} = \boldsymbol{f}_1 \cdot (\boldsymbol{f}_2 \times \boldsymbol{f}_3). \tag{6}$$

Back-rotated counterparts of deformation gradient and strains are specified as

$$\boldsymbol{F}^r = \boldsymbol{Q}^T\boldsymbol{F} = \boldsymbol{I} + \boldsymbol{\gamma}_\alpha^r \otimes \boldsymbol{e}_\alpha^r + \boldsymbol{\gamma}_{33}^r \otimes \boldsymbol{e}_3^r \quad , \quad \boldsymbol{\gamma}_\alpha^r = \boldsymbol{\eta}_\alpha^r + \boldsymbol{k}_\alpha^r \times \boldsymbol{a}^r \quad \text{and} \quad \begin{matrix} \boldsymbol{\eta}_\alpha^r = \boldsymbol{Q}^T\boldsymbol{z}_{,\alpha} - \boldsymbol{e}_\alpha^r \\ \boldsymbol{\kappa}_\alpha^r = axial\left(\boldsymbol{Q}^T\boldsymbol{Q}_{,\alpha}\right). \end{matrix} \tag{7}$$

The plane stress condition is enforced imposing in the equating $(\boldsymbol{\tau}\boldsymbol{e}_3)\cdot\boldsymbol{e}_3 = 0$ and the Piola-Kirchhoff stress tensor is defined as

$$\boldsymbol{P} = \frac{\partial\psi}{\partial\boldsymbol{F}} =: \partial_F\psi = \boldsymbol{\tau}_i \otimes \boldsymbol{e}_i^r \text{ , where } \boldsymbol{\tau} = \frac{\partial\psi}{\partial\boldsymbol{f}_i}. \tag{8}$$

Weak form of equilibrium and Constitutive equations

The weak form of equilibrium equation is implemented in the current model by equations

$$\delta W = \delta W_{int} - \delta W_{ext} = 0 \text{ , } \forall\delta\boldsymbol{u} \qquad \text{and} \qquad \begin{matrix} \delta W_{int} = \int_B \boldsymbol{P}:\delta\boldsymbol{F}dV = \int_{\Omega^r} (\boldsymbol{\sigma}_\alpha^r \cdot \delta\boldsymbol{\varepsilon}_\alpha^r) d\Omega^r \\ \delta W_{ext} = \int_{\partial B} \bar{\boldsymbol{t}}\cdot\delta\boldsymbol{x}dA + \int_B \bar{\boldsymbol{f}}\cdot\delta\boldsymbol{x}dV \text{ ,} \end{matrix} \tag{9}$$

where δw_{ext} and δw_{int} are virtual work of external and internal forces, $\bar{\boldsymbol{t}}$ and $\bar{\boldsymbol{f}}$ are the boundary forces. In previous equation we still have

$$\boldsymbol{\sigma}_\alpha^r = [\boldsymbol{n}_\alpha^r \quad \boldsymbol{m}_\alpha^r]^T \text{ , } \quad \boldsymbol{\varepsilon}_\alpha^r = [\boldsymbol{\eta}_\alpha^r \quad \boldsymbol{\kappa}_\alpha^r]^T \text{ , } \quad \boldsymbol{n}_\alpha^r = \int_H \boldsymbol{\tau}_\alpha^r dH \quad \text{and} \quad \boldsymbol{m}_\alpha^r = \int_H (\boldsymbol{a}^r \times \boldsymbol{\tau}_\alpha^r) dH \text{ , } \tag{10}$$

considering $\boldsymbol{n}_\alpha^r$ and $\boldsymbol{m}_\alpha^r$ as Back-rotated Forces and moments per unit length, $\boldsymbol{\kappa}_\alpha^r$ and $\boldsymbol{\eta}_\alpha^r$ as Back-rotated curvature vector and membrane strains.

The current model uses an elastic material with strain energy defined by

$$\psi = \frac{1}{2}\lambda\left(\frac{1}{2}(\mathrm{J}^2 - 1) - ln(\mathrm{J})\right) + \frac{1}{2}\mu\left(I_1 - 3 - 2ln(\mathrm{J})\right). \tag{11}$$

In the equation above, λ and μ are Lamé coefficients, $\psi(\boldsymbol{F})$ is Helmholtz free energy and $\boldsymbol{C} = \boldsymbol{F}^T\boldsymbol{F}$ is deformation Cauchy-Green (right) tensor. I_i are the invariants of the Cauchy-Green tensor "C".

Finite element definition and Kinkling angle

The finite element has 6 nodes, a quadratic displacement field (Nodal Values $u^{(1)}..u^{(6)}$) and 3 independent scalar rotation parameters ($\varphi_\Delta^{(4)}, \varphi_\Delta^{(5)}, \varphi_\Delta^{(6)}$). Figure 2 illustrates the FE Model.

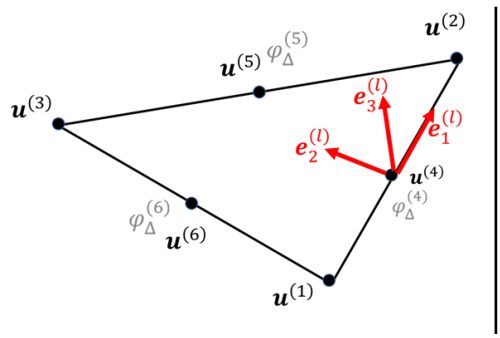

Figure 2. Finite element model. /

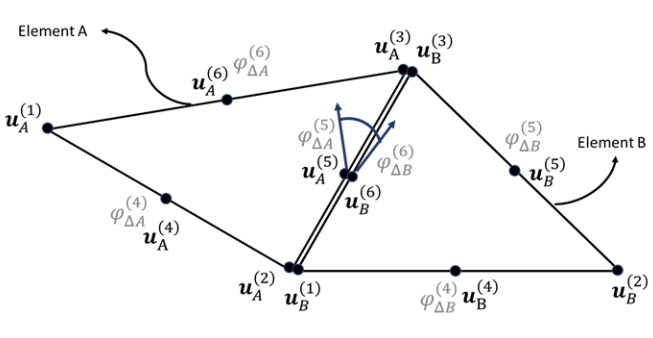

Figure 3. Kinkling angle - Adjacent elements.

The kinkling angle definition is an import part in this Finite Element model. As the kinematics of the shell is based on Kirchhoff-Love theory, the displacement gradient must be continuous in whole domain and consequently the kingling angle between adjacent elements must remain continuous through the deformation. Geometrically the kinkling angle is interpreted as the angle between mid-surface normal of adjacent elements (see Figure 3).

Considering that, the current model imposes a penalty to certain kinematical variables in order to have this C^1 continuity approximated when element size gets refined asymptotically ($h \to 0$)(Viebahn et al. [4]). As expressed in equation (2), $\boldsymbol{Q}$ is the tensor that rotates normal from reference to current configuration. In the

development it is used also Rodrigues rotation parameters, in which $\boldsymbol{Q}$ may be written as a function of $\boldsymbol{\alpha}$:

$$\alpha = 2\tan(\theta/2)\,, \qquad \boldsymbol{\alpha} = \alpha\mathbf{e}\,, \qquad \mathbf{A} = \mathrm{skew}(\boldsymbol{\alpha})\,,$$
$$\widehat{\mathbf{Q}}(\boldsymbol{\alpha}) = \left(\mathbf{I} - \frac{1}{2}\,\mathbf{A}\right)^{-1}\left(\mathbf{I} + \frac{1}{2}\,\mathbf{A}\right) = \mathbf{I} + \frac{4}{4 + \alpha^2}\left(\mathbf{A} + \frac{1}{2}\mathbf{A}^2\right). \tag{12}$$

Rotation increments are easily approached when using Rodrigues parameter considering the equations

$$\boldsymbol{Q}_{i+1} = \boldsymbol{Q}_\Delta \boldsymbol{Q}_i \quad , \qquad \boldsymbol{Q}_{i+1} = \widehat{\boldsymbol{Q}}(\boldsymbol{\alpha}_{\mathbf{i+1}})\,,\ \boldsymbol{Q}_\Delta = \widehat{\boldsymbol{Q}}(\boldsymbol{\alpha}_\Delta)\ ,\ \boldsymbol{Q}_i = \widehat{\boldsymbol{Q}}(\boldsymbol{\alpha}_\mathbf{i}) \quad \text{and}$$
$$\boldsymbol{\alpha}_{\mathbf{i+1}} = \frac{\mathbf{4}}{\mathbf{4} - \boldsymbol{\alpha}_\mathbf{i}\cdot\boldsymbol{\alpha}_\Delta}\left(\boldsymbol{\alpha}_\mathbf{i} + \boldsymbol{\alpha}_\Delta - \frac{\mathbf{1}}{\mathbf{2}}\boldsymbol{\alpha}_\mathbf{i}\times\boldsymbol{\alpha}_\Delta\right). \tag{13}$$

Yet considering kinematical relations (2)(3) and sub-sequential time steps ($\{\boldsymbol{e}_1^i, \boldsymbol{e}_2^i, \boldsymbol{e}_3^i\}$ at t_i and $\{\boldsymbol{e}_1^{i+1}, \boldsymbol{e}_2^{i+1}, \boldsymbol{e}_3^{i+1}\}$ at t_{i+1}), one have applying (13)

$$\boldsymbol{e}_3^{i+1} = \boldsymbol{Q}_\Delta \boldsymbol{e}_3^i\,, \qquad \boldsymbol{e}_3^{i+1} - \boldsymbol{e}_3^i = \boldsymbol{\alpha}_\Delta \times \boldsymbol{e}_3^m \quad \text{and} \qquad \boldsymbol{e}_3^m = \frac{1}{2}\left(\boldsymbol{e}_3^{i+1} + \boldsymbol{e}_3^i\right). \tag{14}$$

In [1], a scalar Rodrigues parameter φ_Δ is presented and one have

$$\boldsymbol{\alpha}_\Delta = \|\boldsymbol{e}_3^m\|^{-2}(\boldsymbol{e}_3^i \times \boldsymbol{e}_3^{i+1}) + \varphi_\Delta\|\boldsymbol{e}_3^m\|^{-1}\boldsymbol{e}_3^m \quad \text{and} \qquad \varphi_\Delta = \|\boldsymbol{e}_3^m\|^{-1}\boldsymbol{\alpha}_\Delta \cdot \boldsymbol{e}_3^m\,. \tag{15}$$

With the equations presented so far, it may be observed that the normal vector $\boldsymbol{e_3}$ for any time step may be determined by the displacement field and consequently by displacement degrees of freedom of the element:

$$\boldsymbol{e_1} = \left\|\boldsymbol{z}_{,1}\right\|^{-1}\boldsymbol{z}_{,1}\ , \qquad \boldsymbol{e}_3 = \left\|\boldsymbol{z}_{,1}\times\boldsymbol{z}_{,2}\right\|^{-1}\left(\boldsymbol{z}_{,1}\times\boldsymbol{z}_{,2}\right)\ , \qquad \boldsymbol{e_2} = \boldsymbol{e_3}\times\boldsymbol{e_1}\ , \tag{16}$$

$$\boldsymbol{u}_{,\mathbf{1}}^{(\mathbf{4})} = \frac{1}{l_3}\left(\boldsymbol{u}^{(2)} - \boldsymbol{u}^{(1)}\right)\ , \qquad \boldsymbol{u}_{,\mathbf{1}}^{(\mathbf{5})} = \frac{1}{l_1}\left(\boldsymbol{u}^{(3)} - \boldsymbol{u}^{(2)}\right)\ , \qquad \boldsymbol{u}_{,\mathbf{1}}^{(\mathbf{6})} = \frac{1}{l_2}\left(\boldsymbol{u}^{(1)} - \boldsymbol{u}^{(3)}\right)\ , \tag{17}$$

$$\boldsymbol{u}_{,\mathbf{2}}^{(\mathbf{4})} = \left(\frac{C_1}{2A}\right)\boldsymbol{u}^{(1)} + \left(\frac{C_2}{2A}\right)\boldsymbol{u}^{(2)} + \left(\frac{C_3}{2A}\right)\boldsymbol{u}^{(3)} + \left(\frac{-C_3}{A}\right)\boldsymbol{u}^{(4)} + \left(\frac{C_3}{A}\right)\boldsymbol{u}^{(5)} + \left(\frac{C_3}{A}\right)\boldsymbol{u}^{(6)}\ ,$$
$$where\ C_1 = x_3 - x_2\,, C_2 = x_1 - x_3\,, C_3 = x_2 - x_1\ . \tag{18}$$

Knowing the local base system at the time step t and t+1, one can define the Rodrigues incremental vector $\boldsymbol{\alpha_\Delta}$ and consequently ϕ_Δ by

$$\boldsymbol{\alpha_\Delta} = \frac{2\left(\boldsymbol{e}_\boldsymbol{j}^\boldsymbol{i} \times \boldsymbol{e}_\boldsymbol{j}^{\boldsymbol{i+1}}\right)}{1 + \boldsymbol{e}_\boldsymbol{k}^\boldsymbol{i}\cdot\boldsymbol{e}_\boldsymbol{k}^{\boldsymbol{i+1}}}\ , \qquad \phi_\Delta = \boldsymbol{\alpha_\Delta}\cdot\frac{\boldsymbol{e_1^m}}{\|\boldsymbol{e_1^m}\|} \quad and \qquad \boldsymbol{e_1^m} = \frac{1}{2}\left(\boldsymbol{e_1^i} + \boldsymbol{e_1^{i+1}}\right)\ . \tag{19}$$

With the equations stated above, it is used a penalty parameter to enforce the approximation between ϕ_Δ and φ_Δ.

$$\Pi^{pen} = \psi + \frac{1}{2}k\left(\varphi_\Delta^{(4)} - \phi_\Delta^{(4)}\right)^2 + \frac{1}{2}k\left(\varphi_\Delta^{(5)} - \phi_\Delta^{(5)}\right)^2 + \frac{1}{2}k\left(\varphi_\Delta^{(6)} - \phi_\Delta^{(6)}\right)^2\ . \tag{20}$$

Here in this text, it is used similar letter in order to illustrate that ϕ_Δ and φ_Δ are concepted to be the same identity but as they are obtained from different variables, thay will in most of the cases have different values. Herein they are forced to approximate numerically by applying the penalty strategy. In other worlds, penalty is used to enforce compatibility of the displacement field and the rotation degree of freedom φ_Δ which is shared between adjacent elements. With this penalty imposed, it is expected to approximate the C^1 continuity condition at element borders with sufficient mesh refinement. The only artificial parameter in the element model is therefore k, which by means of simulation has been defined as a multiple of the bending stiffness of a shell ($Eh^3/\left(12(1-\nu^2)\right)$).

3 RESULTS

The element model developed in this article has been implemented in a numerical environment and have been simulated for different conditions in order to compare its results to other finite element models available. The two simulation scenarios that are presented in this article are "Cantiliever Beam" and "Pinched cylinder". The simulations have been executed numerically in three (3) different numerical enviroments. First, with the model developed in this article (KL T63i Pen). Second using the model developed in Costa e Silva [5] (KL T63i Lag). Third, using commercial software (Autodesk Nastran – Ctria6 element. See Autodesk [10]).

Cantilever Beam

In this classical structural problem, a beam (in this case a narrow shell) is clamped at one side and is free but subject to a bending force in the other side (see Figure 4). The following list represents the simulation parameters:

- $\mathrm{E} = 210 \cdot 10^9\ Pa$;
- $\nu = 0{,}3125$;
- $L\ (beam\ length) = 2400\ mm$;
- $h(cross\ section\ height) = 100\ mm$;
- $b(cross\ section\ width) = 11{,}64\ mm$;

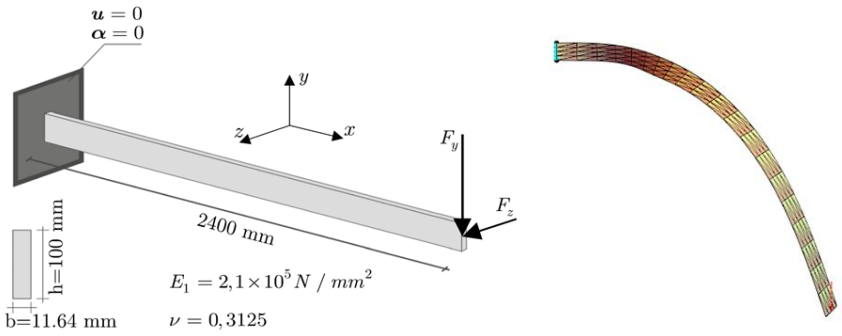

Figure 4 - Cantilever Beam

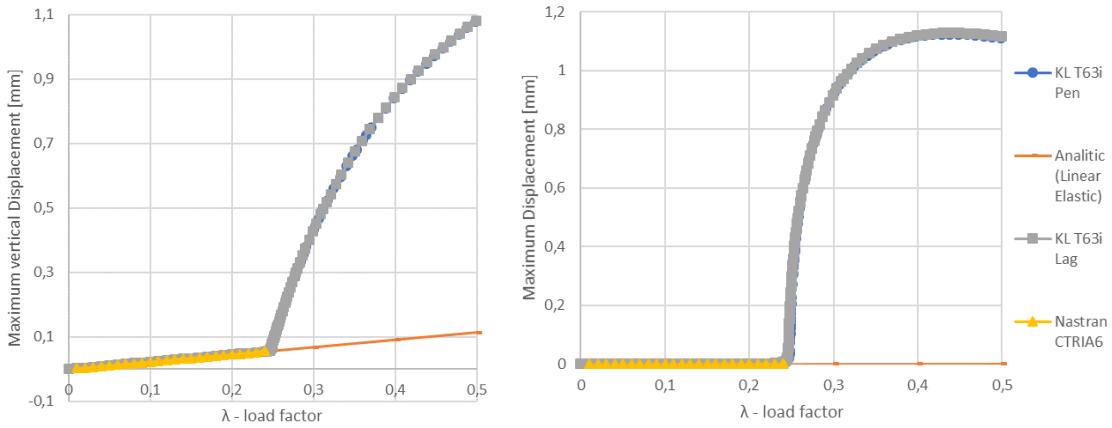

Figure 5 – Vertical and lateral maximum displacement vs load factor.

Figure *5* plots the vertical and lateral displacement of the free side of the beam. It can be seen that for load factor bigger than 0,25 the beams buckles. In this scenario, Lagrange and penalty based models behave practically the same results (displacements). Also, for load factor bigger than 0,25, the Nastran model could not converge, which demonstrate its limitation for thin shells high nonlinear simulations.

Pinched Cylinder

This simulation scenario has been based on the articles (Ivannikov et al. [11], Campello et al. [3], Sansour and Kollmann [12] and Costa e Silva[5]). Here, a thin cylinder is subject to a radial vertical force in its center (see Figure 6). The parameters of the simulation are the same that in bibliography:

- $\mathrm{E} = 3 \cdot 10^{10}\ Pa$;
- $L\ (Cylinder\ length) = 200\ mm$;

- $\nu = 0{,}3$
- $F\ (force)\ =\ 1000\ N$
- $R(Cylinder\ Radius)\ =\ 100\ mm;$
- $b(thickness)\ =\ 1\ mm;$

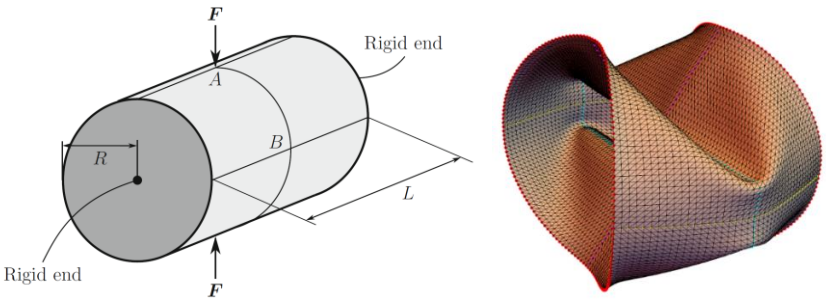

Figure 6 – Pinched cylinder

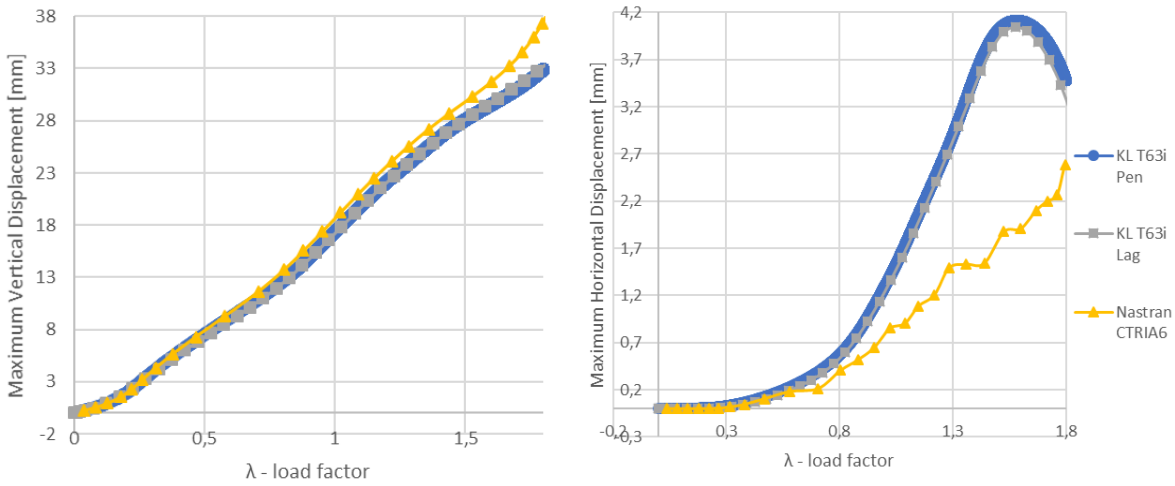

Figure 7 - Maximum vertical displacement at A; Maximum Horizontal displacement at B

It can be seen on Figure 7 that Nastran have generated different results, less smooth and stiffer compared to the KL T63I (Penalty and Lagrange), showing its limitation in this type of simulation. In contrast, KL models have presented compatible, smooth and coherent results.

4 Conclusions

The text herein presented demonstrates the most important aspects of the kinematical model and the two simulated scenarios demonstrates coherent and satisfactory results. Further tests and benchmarks are going to be presented in further work. It is believed that powerful triangular mesh generators combined with the model developed in this article might be a good alternative for simulating thin nonlinear shell in finite element methods.

Acknowledgements. Matheus L. Sanchez thankfully acknowledges Clark Solutions, where he works as a project engineer providing financial support, knowledge, applicability and industrially experience. C. Costa e Silva gratefully acknowledges the Federal Institute of Science and Technology Education of São Paulo for financial support. P. M. Pimenta acknowledges the support by CNPq under the grant 308142/2018-7 and the Alexander von Humboldt Foundation for the Georg Forster Award that made possible his stays at the Universities of Duisburg-Essen and Hannover in Germany as well as the French and Brazilian Governments for the Chair CAPES-Sorbonne that made possible his stay at Sorbonne Universités on a leave from the University of São Paulo.

Authorship statement. The authors hereby confirm that they are the sole liable persons responsible for the authorship of this work, and that all material that has been herein included as part of the present paper is either the property (and authorship) of the authors, or has the permission of the owners to be included here.

References

[1] Simo J.C., Fox, D.D., "On a stress resultant geometrically exact". Comput Methods Appl Mech., 1989.
[2] Pimenta, P.M., "On the geometrically-exact finite-strain shell". Proceeding of the third Pan-American congress on., 1993.
[3] Campello, E.M.B.; Pimenta, P.M.; Wriggers, P. "A triangular finite shell element based on a fully nonlinear shell formulation". Computational Mechanics. Comput. Methods Appl. Mech. Engr, 2003.
[4] Viebahn, N.; Pimenta, P.M.; Schröder, J.A., "A simple triangular finite element for nonlinear thin shells: statics, dynamics and anisotropy". Computational Mechanics, 2017.
[5] Costa e Silva, C., "Geometrically exact shear-rigid shell and rod models". Ph.D. Thesis, University of Sao Paulo, Brazil, 2020.
[6] Sanchez, M.L.; Costa e Silva, C; Pimenta, P.M., "A simple fully nonlinear Kirchhoff-Love shell finite element". LAJSS, to be published
[7] Reddy, J. N., "Theory and analysis of elastic plates and shells". CRC press, 2006.
[8] Pimenta, P.M, Campello, E.M.B.,"Shell curvatures as an initial deformation: a geometrically exact finite element approach". Int J Numer Methods Eng 78:1094–1112, 2009
[9] Pimenta, P.M., Neto, E.S.A, Campello E.M.B., "Fully Nonlinear Thin Shell Model of Kirchhoff-Love type", 2010.
[10] Autodesk, Inc CTRIA6 Autodesk Nastran. "https://knowledge.autodesk.com/support/nastran/learn-explore/caas/CloudHelp/cloudhelp/2020/ENU/NSTRN-Reference/files/GUID-956704D9-26C5-4FF8-85F2-955F383C5ECD-htm.html", 2019.
[11] Ivannikov, V., Tiago, C., Pimenta P.M., "Generalization of the C1 TUBA plate finite elements to the geometrically exact Kirchhoff–Love shell model". Comput Methods Appl Mech Eng, 2015
[12] Sansour, C., Kollmann, F., "Families of 4-node and 9-node finite elements for a finite deformation shell theory. An assessment of hybrid stress, hybrid strain and enhanced strain elements". Comput Mech 24:435–447, 2000